iJRASET
International Journal For Research in Applied Science and Engineering Technology

INTERNATIONAL JOURNAL FOR RESEARCH

IN APPLIED SCIENCE & ENGINEERING TECHNOLOGY

Volume: 9 **Issue:** XI **Month of publication:** November 2021

DOI: https://doi.org/10.22214/ijraset.2021.39127

www.ijraset.com

Call: 08813907089 | E-mail ID: ijraset@gmail.com

International Journal for Research in Applied Science & Engineering Technology (IJRASET)
ISSN: 2321-9653; IC Value: 45.98; SJ Impact Factor: 7.429
Volume 9 Issue XI Nov 2021- Available at www.ijraset.com

A Recent Progress in Performance and Property Improvement in Underwater Welding

Ayush Bakrewal[1], Aldrin Antonio Agostinho Fernandes[2], Kiiran Jadhav[3], Siddesh Sutrave[4], Atishay Jain[5]
[1, 2, 3, 4, 5]*Department of Mechanical Engineering, Vellore Institute of Technology, Vellore*

Abstract: ***Underwater welding is the process of connecting materials underwater in the presence of water. It is used to maintain and improve the structure in marine and offshore applications. It's utilized for underwater pipeline maintenance, submerged offshore oil drilling, and ship repairs. It can also be found in nuclear power plants and deep-sea mining. Underwater welding is divided into two categories dry welding and wet welding. Dry welding entails enclosing the weld zone in a hyperbaric tank filled with a gas mixture and welding at the prevailing pressure. Wet welding is a type of welding that uses waterproof electrodes and is done directly on the component to be welded. The major benefit of this welding is its simplicity and cost effectiveness, but we can't obtain high weld quality as easily as we can with dry welding. Dry welding, on the other hand, may provide high weld quality, but it is a time-consuming procedure that needs the welder to secure the region with the hyperbaric vessel, and it is also a costly method. Underwater welding has a number of issues, including bubble arc generation, cold cracking, microstructural deformation, and more. We attempted to bring together the most recent developments in the field of underwater welding. We've outlined several techniques that were used to improve welding characteristics as well as important issues that must be addressed. This review article may be used to figure out what measures need to be taken to enhance the underwater weld joint quality.***

Keywords: Underwater welding, underwater wet welding, underwater dry welding, hyperbaric vessel, underwater welding development.

I. INTRODUCTION

Underwater welding is used in underwater pipeline maintenance and repairs, naval projects, and marine and offshore applications. It is critical in nuclear power plants, deep sea mining, and submerged offshore oil drilling because they are prone to corrosion, constructional difficulties, material fatigue, unknown variables, assembly issues, and operational overload that require maintenance and repair.

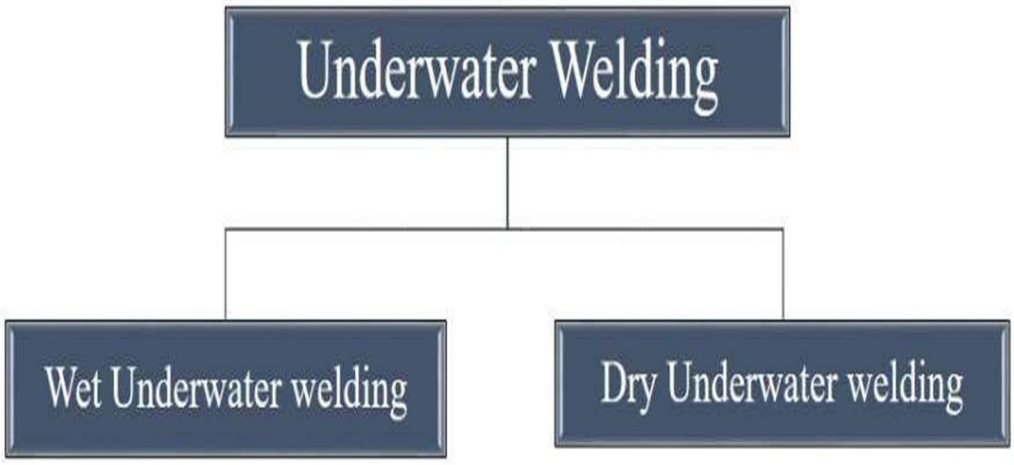

Fig. 1 Classification of underwater welding

Wet underwater welding (W-UWW) and dry undersea welding (D-UWW) are the two major categories of underwater welding (D-UWW). In comparison to underwater dry welding, which has a sophisticated operation setup as well as less operational space for the diver, underwater wet welding is of utmost importance because it has a low cost of operation, easy operational setup with free degree of movement for the diver, high production efficiency, and a simple device. As a result, several studies in the field of underwater wet welding have been performed to address this issue [30].

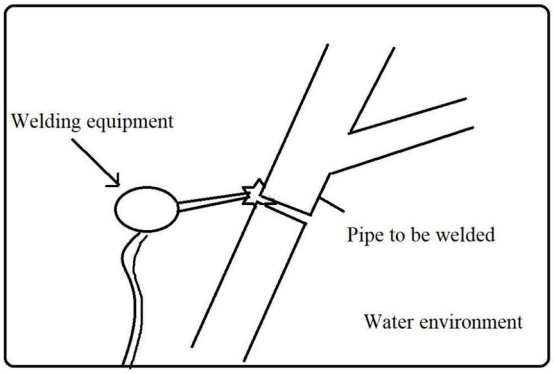

Fig. 2 Underwater wet welding

Underwater welding procedures are executed based on the material to be welded, the welder's competence, the cost of operation, and water variables such as water velocity, temperature, and so on. Welding procedures are simple to implement. Shielded Metal Arc Welding (SMAW), Flux-cored Arc Welding (FCAW), and Gas Tungsten Arc Welding are examples of these types of welding (GTAW). Shielded Metal Arc Welding (SMAW) is a method of melting the work piece and electrode using heat generated by an electric arc discharge [43]. Flux shields the electrode, and the filler metal deposits as slag on the material, protecting the weld zone throughout the cooling process. FCAW (Flux Cored Wire Arc Welding) is a welding process in which flux is utilized as a shielding layer and alloying elements are added to the welding metal placed on the electrode. FCAW is simple to use and can be done in any position. TIG (Tungsten Inert Gas Welding) or GTAW (Gas Tungsten Arc Welding) is a welding technology that employs tungsten electrode and filler metal that are introduced separately to the welding process. Suitable for low-welding-performance metals and alloys. Because it utilizes a little current, it generates a steady arc [43].

Even though underwater wet welding (UWW) provides a number of advantages, such as smaller equipment, more mobility, reduced preparation time, and lower costs. However, the drawbacks of UWW, such as lower material ductility, increased material hardness in the Heat Affected Zone (HAZ), weld metal flaws, unstable arc flames, and water waves surrounding the welding region, are rapidly becoming apparent. It must be rectified since it will have an impact on underwater welding results, such as fracture propagation, excessive porosity, and poor welding performance, as well as lower mechanical characteristics of the weld joint [64] The magnitude of the water waves near the underwater welds fluctuates continually throughout the application of underwater welds, resulting in periodic stresses on the material structure. In addition, the material's structure will be unfavorable. Furthermore, a significant number of welding inclusions might speed up the formation of fatigue cracks.

Porosity and inclusions become a problem when the structure ages. Porosity causes hydrogen trapping, which can then lead to hydrogen embrittlement, which causes damage in the form of fractures and decreases the structure's dependability.

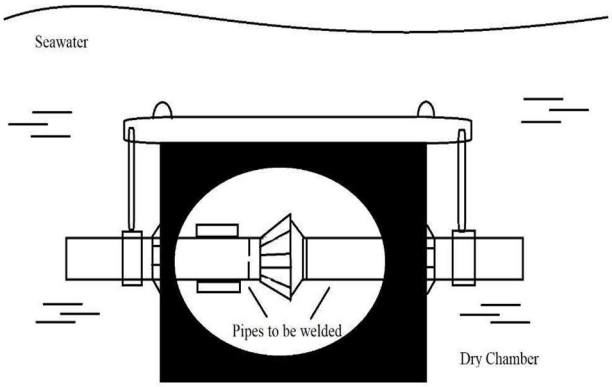

Fig. 3 Underwater dry welding

Underwater dry welding entails setting up a dry chamber inside the water to produce a dry environment as shown in the fig 1.3.

Based on the aforementioned issues, a thorough investigation of the failures has been conducted, as well as the actions that must be taken to improve weld quality. This review article will serve as a resource for tracking recent advancements and developments in the field of underwater welding. It will also make recommendations on how to enhance the weld performance [30]

ISSN: 2321-9653; IC Value: 45.98; SJ Impact Factor: 7.429
Volume 9 Issue XI Nov 2021- Available at www.ijraset.com

II. LITERATURE REVIEW

Welding parameters are the most significant and decisive element in welded joint quality. Guo et al. discovered a link between the arc voltage and welding current in the UWW method and the kind of metal transfer. In UWW, I investigated the effects of heat input and metal transport on weld shape and microstructure. Furthermore, Wierczyska et al. [28] investigated the effect of welding settings on the diffusible hydrogen concentration of UWW deposited metal. When welding settings were modified, Mendonça and Bracarense looked at the link between formation frequency and bubble size. They came to the conclusion that the bubble diameter might be improved. Control welding settings to improve arc protection. Many researchers pay special attention to the welding speed as one of the welding processes factors since it has a significant impact on the welding process and weld quality (especially for UWW). Guo et al. investigated the effect of welding speed on the UWW transfer mode and discovered that a faster welding speed favors the repelling wide-angle transfer mode. [59] Wang et al. Bubble reliance on dynamic welding speed was investigated. They discovered that when the welding speed increases, the shape of the bubble changes, affecting the process's stability. As a result, it is clear that the welding speed has a significant impact on the molten pool's dynamics. As a result, the weld pool's dynamic behavior is investigated. UWW was tested at various welding speeds in the current study, and the connection between welding speed and welding dynamics, weld formation, and diffusible hydrogen concentration was assessed on this basis [13].

Arc welding is the most frequent underwater welding process. However, fracture sensitivity, high hydrogen diffusivity, and poor arc stability in wet and local dry welding are difficulties connected with underwater arc welding, which limit its growth. According to recent research, underwater laser welding is considerably more beneficial than traditional welding [2]. A protective substance is added to the base metal in advance of underwater laser wet welding to raise the depth of the welded water to 20 mm. The water around the laser irradiation region must be eliminated in order to achieve high-quality welds under typical water depth using underwater laser welding [78]. As a result, the method of underwater dry spot laser welding has been investigated. During the underwater laser welding process, Zhang et al. scanned the optical signal in the nearby drying cavity, and the results revealed that the infrared signal indicated protection. Sano et al. used local underwater dry laser welding technology to successfully apply an anti-corrosion coating to the surface of underwater components. Underwater dry local laser welding, as demonstrated by Yoda et al., may resist stress corrosion cracking in underwater components [52]. Guo et al. looked at butt joints that were welded underwater utilizing local laser welding. Their findings revealed that pore flaws induced by water vapor impaired the mechanical characteristics of the butt joint, and owing to the cooling action of water, ferrite formed in the center of the weld.

The frictional stir welding technique has a lot of advantages for alloys that have a negative relationship between weld quality and welding temperature. Many of these alloys have a high precipitating property in the weld zone, making them brittle and porous weld zones prone to formation [10].

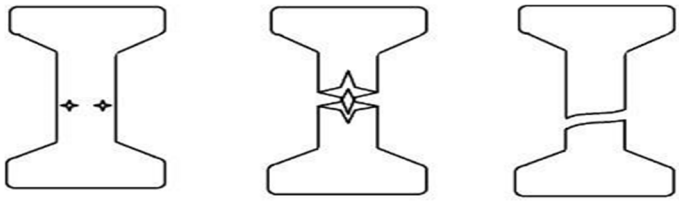

Fig. 4 Crack initiation, propagation and fracture

The frictional stir welding technique has a lot of advantages for alloys that have a negative relationship between weld quality and welding temperature. Many of these alloys have a high precipitating property in the weld zone, making them brittle and porous weld zones prone to formation [10]. Underwater laser welding keyhole and weld pool are studied using a mathematical framework. The behavior of the weld pool and keyhole at the same time in terms of laser depth and strength will be addressed later. The heat and mass transport characteristics of underwater laser welding is discussed. When a weld pool comes into touch with water, it cools rapidly, resulting in a new morphology. Furthermore, as the depth of the water increases, the temperature of the keyhole rises. To analyze the fatigue behavior of welded steel, elements such as water depth, water waves, and temperature are taken into account. Water waves and depth can have a significant impact on the welding current and arc stability. The development of fine microstructure is caused by the rapid cooling of the weld zone, decreasing the impact strength of the welded component. Post-weld heat treatment is recommended to combat this. Diverse materials are welded underwater. The mechanical properties and microstructural features of AA2519-T87 Aluminum alloy joints produced by underwater friction stir welding are investigated. The cooling system is good because the welding is done under water, thus grain coarsening and precipitation are significantly decreased, resulting in higher joint strength [99].

ISSN: 2321-9653; IC Value: 45.98; SJ Impact Factor: 7.429
Volume 9 Issue XI Nov 2021- Available at www.ijraset.com

III. EXPERIMENTAL PROCEDURE

Table 1 lists the composition and mechanical characteristics of the austenitic 304 stainless steel utilized in this test. The filler rod is a 1.6 mm diameter self-shielded flux-cored wire made of CaF2- Al2O3 slag, which is the most sophisticated unique flux cored wire for UWW. Positive direct current electrodes were used in the UWW studies (DCEP). Figure 2 shows the welding settings. Other variables were maintained constant while welding speed was altered [77].

Table I
Welding Process Parameter

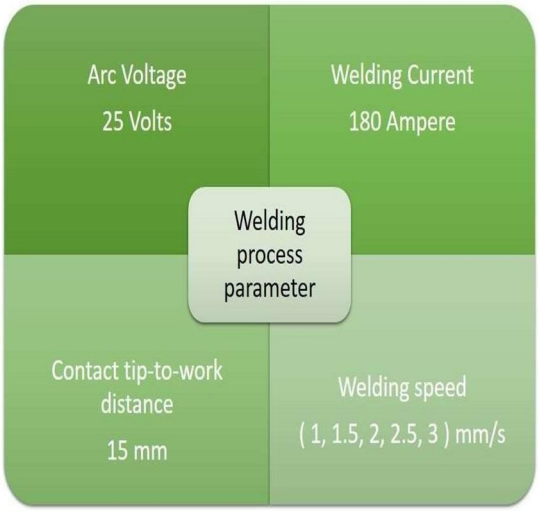

The experiment was carried out using an X-ray system, with the base metal held securely in place and high-resolution pictures of the weld pool taken using a high-speed camera. To compute the movement of the weld pool, a technique was devised that recorded the fluctuation in height from a fixed location [82].

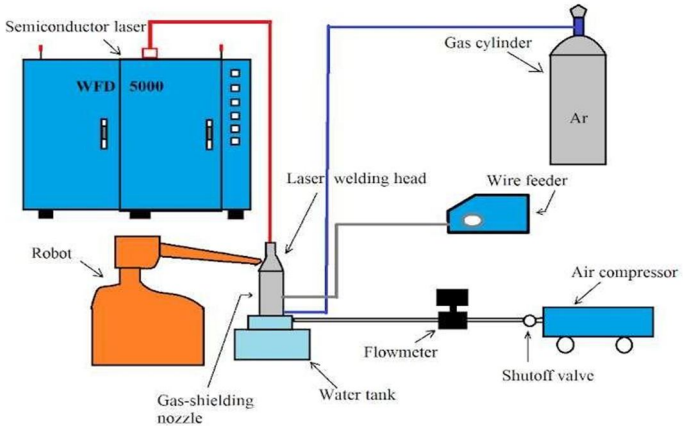

Fig. 5 X-ray analysis of underwater laser welding

A semiconductor laser with a wavelength of 915 nm was utilized in this experiment. The experiment was carried out with the assistance of a 6-axis robot. To establish a local dry cavity and safeguard the laser welding section in a water environment, a self-designed shielding gas nozzle was employed. Argon was utilized as a shielding gas. The outer nozzle's diameter and height were 120 and 110 mm, respectively, while the inner nozzles were 40 and 85 mm. A wire feeder injected the wire, and a shielding gas nozzle positioned the wire tube at a 30-degree angle in the front feed direction [77].

The base metal was a cold rolled stainless steel plate that was submerged in water during underwater laser welding, and the filler wire was a 1.0 mm diameter 304 stainless steel wire [82].

ISSN: 2321-9653; IC Value: 45.98; SJ Impact Factor: 7.429
Volume 9 Issue XI Nov 2021- Available at www.ijraset.com

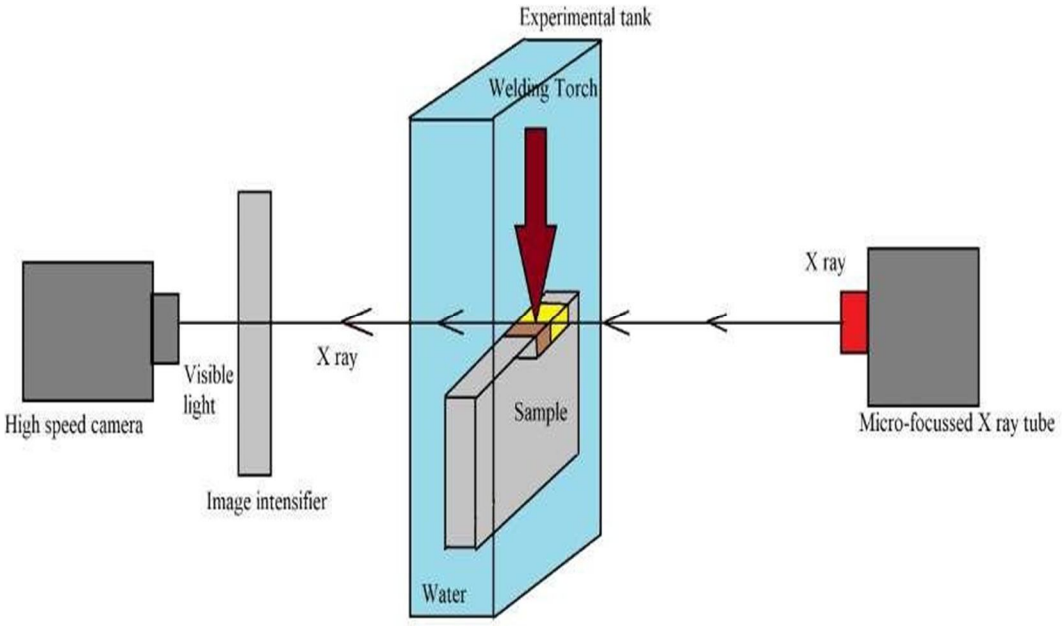

Fig. 6 Schematic diagram of underwater filler wire laser welding system

In a water and air environment, a 2 mm thick 6061 aluminum alloy was friction stir spot welded at varied tool speeds of 700, 900, and 1100 RPM.

Welding is done utilizing a TiO2-Fe2O3 system with a diameter of 1.6 mm. Base metals and freight have different chemical compositions. 30 V, 5 m/min, or 2 mm/s are the welding voltage, wire feed speed, and welding speed. The contact to working element distance (CTWD) is 20 mm, while the cable extension length is 15 mm. The connection between arc bubble behavior and droplet transport is studied using X-ray imaging.

A micro-focus X-ray tube, an image transducer that transforms the emitted X-ray picture into a visible image, and a high-speed camera (2000 images per second) make up the in-situ X-ray imaging system [114].

Options for high-speed for recording, a CR series camera with a 256256-pixel chip is utilized. 130 kV and 0.3A are the X-ray source's specifications. Extract and analyze continuous video pictures of droplet movement and bubble activity using wet welding [122].

IV. RESULTS AND DISCUSSION:

A. Weld Pool

With varied welding speeds ranging from 1mm/s to 3mm/s, the dynamic behavior of the weld pool was studied. It was discovered that a droplet transfer procedure was taking place. The flow of gas in the weld pool and droplet hits produce variations in the molten pool. The droplets are a major contributor to the gas in the weld pool [11]. When liquid metal flows in the weld pool tails, the temperature of the liquid metal drops dramatically, resulting in gas entrapment.

A huge amount of hydrogen was originally held in the liquid metal, which then attempted to exit the surface when the temperature dropped dramatically, reducing the gas solubility.

As a result, each droplet causes gas to accumulate in the weld pool [11].

The provided problem was handled by doing the experiment at various welding speeds, and the following findings were made: when the welding speed rises, the length of the molten pool steadily grows, reducing the molten pool's strength [61].

The strength of the weld seam, on the other hand, steadily diminishes as the welding speed increases. Large bubbles become harder to produce. As a result, variations in the molten pool are considerably minimized. These two factors combine to lessen the standard issue, and as welding speed increases, the vibration of the molten pool reduces [9]

B. Nozzle Gas Flow Rates

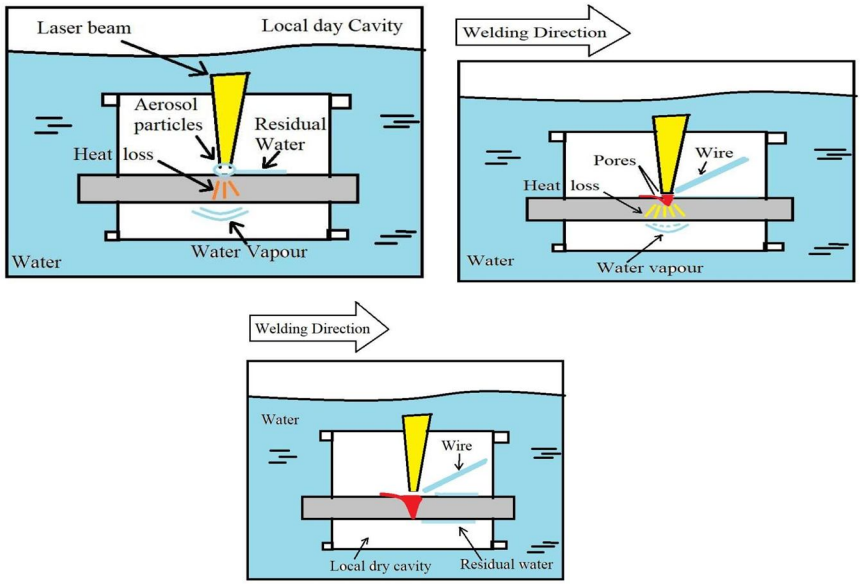

Fig. 7 Underwater filler wire laser welding process at different gas flow rates: (a) initial stage at 0 L/min gas flow rate, (b) stable stage at 0 L/min gas flow rate, (c) welding process at 30 L/min gas flow rate.

The impact of the flow rate of the return flow from the nozzle, the travelling speed, and the wire feeding speed on the surface appearance, as well as the mechanical characteristics of the welding connection, were studied in order to achieve a high-quality butt junction [89]. Underwater laser welding was carried out on the upper surface of the butt joint using a single sided gas-shielding nozzle at various gas flow rates. The impact of displacement rate on weld formation and weld cross section is investigated using an optimum return air flow rate (50 l/min) and wire feeding speed of 50 mm/s [116].

C. Microstructural Composition For Different Materials

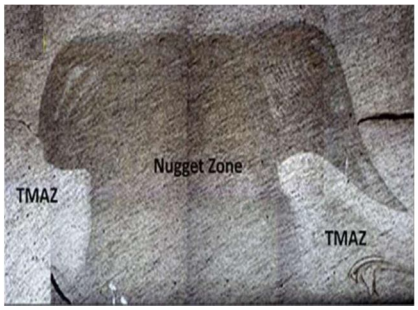

Fig. 8 Microstructural cross-sectional view of friction stir spot welding (FSSW)

To begin with, some types of weld zones with ripples in them have been noticed as they move away from the axis. Second, there are certain zones on the specimen that are neither too close nor too far away from the axis; these zones suffer some mechanical deformation and temperature impact, but are not greatly affected. Finally, there are zones that are impacted thermally but not mechanically. Fourth, any mechanical or thermal changes have no effect on the base metal [135].
Because the rate at which heat is generated in friction stir spot welding (FSSW) is significantly higher than in thermo mechanical affected zone (TMAZ), both in the tool pin and shoulder area, the grain size is seen to be more refined [145].
There are a variety of ways to improve the quality of underwater welding, including heat treatment. Heat treatments, such as preheating and post-weld heat treatment, are extremely helpful in improving weld quality. The microstructure of the weld region is homogenized after heat treatment. Heat treatment after the weld prevents the material from breaking. Many elements influence the quality of a weld, including the depth at which it is performed, the humidity in the welding region, and the arc stability supplied throughout the welding process.

The size of these processes can have an impact on the size of faults. The size of ferrite microstructures in the weld region grows as a result of post-weld heat treatment [66]In a water and air environment, a 6061-aluminium alloy with a thickness of 2 mm was friction stir spot welded at varied tool speeds of 700, 900, and 1100 RPM.

As welding takes place in water, the weld zone is subjected to rapid cooling, resulting in microstructural refinement and increased strength when compared to welding on land [93].

AA2519-T87 The mechanical properties and microstructural features of aluminum alloy joints produced by underwater friction stir welding are studied. The cooling system is good since the welding is done under water; thus, grain coarsening and precipitation are significantly minimized, resulting in higher joint strength. The thermal mechanical impacted zone seen in FSW is substantially decreased in UWFSW, resulting in low and consistent heat input along the weld line, resulting in grain coarsening and precipitate formation [99].

D. Advanced Welding Techniques

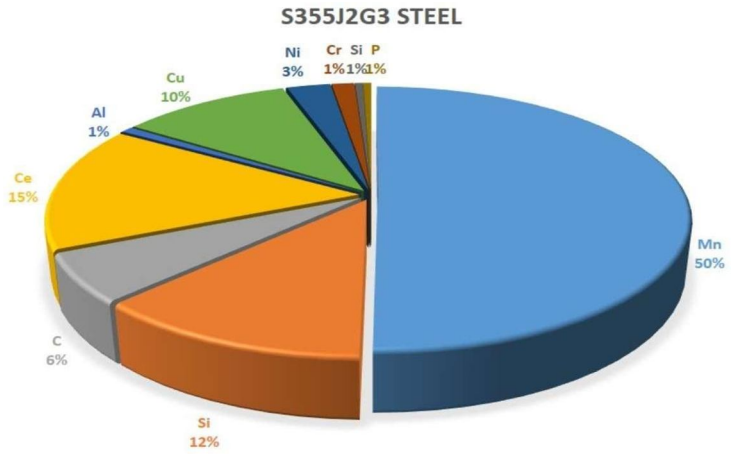

Fig.9 %Wt. composition of S355J2G3 steel

In Friction Stir welding, heat input is critical for dynamic crystallization. At low rotating speeds or high welding speeds, grain size is regulated by strain rate, whereas at high rotational speeds or low welding speeds, grain size is controlled by heat [61].

Table II
HY 100 STEEL, S355J2 + N STEEL And 316TI STEEL (WT. %) Chemical Composition

Element	HY 100 steel (wt %)	S355J2 + Nsteel (wt %)	316Ti steel (wt %)
C	0.14	0.12	0.04
Si	0.23	0.34	0.42
Mn	0.31	1.4	1.5
P	0.01	2.01	0.03
S	<0.01	<0.01	<0.01
Cr	1.5	0.04	16.9
Ni	2.9	0.14	10.8
Mo	0.44	0.01	2.0
Al	0.04	0.03	-
Cu	0.01	0.18	0.31
Co	-	-	0.12
Ti	-	-	0.38
V	-	-	0.10
W	-	-	0.10

Table III
Mass Measurements Of Welded Steel

Exposure period (hours)	HY 100 welded steel specimen (gr)	S255J2 + N welded steel specimen (gr)	316Ti welded steel specimen (gr)
0	7298	6281	7555
24	7301	6284	7556
48	7303	6287	7556
72	7305	6290	7557
96	7310	6305	7556
168	7313	6307	7557
192	7318	6309	7557
216	7319	6314	7557
240	7322	6318	7557
264	7326	6320	7557
After 300h exposure and removal of corrosion products	7264	6218	7556

Table IV
Mass loss of each welded specimen after the integration of the salt spray test.

Mass loss	HY 100 welded steel specimen (gr)	S355J2 + N welded steel specimen (gr)	316Ti welded steel specimen (gr)
Initial mass before exposure (W1)	7298	6281	755
Mass after 300 h exposure and removal of corrosion products (W2)	7264	6218	7556
Mass loss (W1-W2)	34	63	negligible

The maximal tensile strength is directly proportional to grain size. The corrosion of HY 100 and S355J2+ N welded steels is pitting, but the corrosion of X6CrNiMo17-12–2 (316Ti) austenitic stainless welded steel is exfoliation. Residual stress, stress concentration, corrosion, temperature, maximum tensile stress, metallurgical structure, and material overload all play a role in weld fatigue failure. Pre-weld heat treatment has been recommended to reduce failure [35].

Dry welding is more expensive than wet welding since it necessitates the use of a hyperbaric tank, but it is also more precise. Wet welding, on the other hand, is considerably less expensive but creates a low-quality weld. It's ideal for repairs. Underwater friction stir welding solves the difficulties of excessive heat input and grain coarsening in friction stir welding. Because of the improved cooling mechanism, precipitation production is significantly decreased [69].

When doing underwater laser welding, the weld pool cools more quickly than the other components, resulting in a new morphology. With increasing depth, the temperature of the keyhole tends to rise. In the case of Friction Stir welding, it has been shown that the weld zone cools more quickly, resulting in novel morphology and grain refinement, resulting in increased strength. The development of delta and gamma ferrite dual phases reduces the fatigue behavior of stainless steel in borated and polluted water [46].

The border between the two phases contributes to hydrogen trapping and the beginning of fractures. Any material's hardening process can be greatly influenced by continuous and repeated fatigue cycles. Timing and fatigue cycles are important factors in hardening [98].

The mathematical model proposed in this work may be used to analyze the fatigue of any reactor component. We can get a better weld in underwater laser welding if we utilize a filler wire and a double side gas nozzle that can generate a local air cavity. The heat-affected zone (HAZ) is reduced by the water [18].

Table V
Chemical Composition of HJ350(WT.%)

Sio2	CaO	Al2O3+ MnO	CaF2	FeO	S	P
30-35	10-20	27-37	14-20	<=1.0	<=0.06	<=0.08

If the weld is being affected by abrupt water currents and disturbances, a 4:6 weight ratio of biphenyl- epoxy resin and welding flux might be used. This combination preserves the weld and aids in the production of a better weld. In high temperatures, the fatigue strength of dissimilar metals is greatly diminished. Water that has been borated or disputed raises it even more. Residual strain can be detected at the welding contact between two different materials, which can lead to dip cracking [147].

Table VI
Chemical Composition of HJ350(WT.%)

CaF2 content	Fe	Cr	Mn	Mo	Al
0%	38.17	11.02	6.63	3.49	1.62
35%	15.54	5.10	4.24	2.37	0.53
60%	12.45	3.38	2.64	1.51	0.29

The weld joint was tested for microstructural features and mechanical qualities using various wires with varying CaF2 concentration. In welding, the weld speed and angle are extremely important. The length of the weld pool grows as the weld speed rises, but the time it takes to solidify and alter the weld pool decreases. The angle of the weld pool determines the form of the pool. Electrodes with polymer coatings were chosen over traditional electrodes for greater penetration power [67]. The application of DCEP polarity decreases hydrogen infusibility. The results of the tests to determine the diffusible hydrogen reveal that the hydrogen in the weld metal ranges from 5 to 21 ml / 100 g Fe and is dependent on the welding conditions, particularly the weld metal consumption. Welds produced using local drying chambers function better than wet welds and can fulfil classification society parameters for depths of up to 200 meters [17] [59].

All electrodes are waterproofed with varnish, with a coating thickness of 0.2 mm on average. Ten different types of electrodes were tested for arc stability, metal transfer, and welding performance. The molten metal lowers and fills with air as the arc travels along the weld. However, this is due to the cooling rate. The metal hardens and produces mounds and deep incisions when welded underwater [54].

We can assure high welding quality without the dangers associated with basic arc welding by utilizing a properly insulated electrode for underwater welding. If this study continues, we can calculate the welding speed [60] to get the optimal strength of the underwater welded connection. Underwater welds have stronger strength and lesser ductility, according to experimental evidence.

Underwater weld strength rose from 6.9% to 41%, but ductility of most welds decreased by roughly 50%. Basic steel material, welding direction, and corrosion of basic steel material are all part of the study. The phase content of marten site (M) and upper bainite (BU) phases reduces as the induction heating voltage increases, whereas the phase content of hypo eutectoid ferrite (PF) and cycloferrite (AF) phases increases. [8] As the heating voltage grows, the temperature rises as well.

E. Graphical Analysis of Weld Zone

Wet solderability has been enhanced thanks to recent developments in nickel-based flux core fillers, and a halogen-free flux formulation for wet soldering has been particularly created. For the actual implementation of the Gas Tungsten Arc Welding (GTAW) process in the over pressure mode, the particular relationship diagram of the service life of the electrodes WL 10 & WT 20 with ambient pressure & arc power is extremely significant. Arc current and voltage are both selected. Because it is high in low ionization elements like potassium and sodium, liquid glass is an essential arc stabilizer and surfactant.

The welding arc is more stable, and the underwater welding process window is more stable, thanks to the density and low ionization potential around the underwater arc.

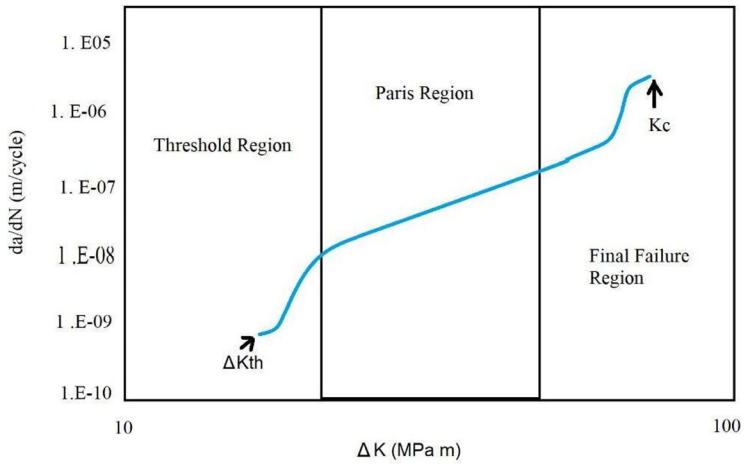

Fig. 10 da/dN vs delta K curve

To scale the fatigue propagation rate in the welded material, a graph of da/dN against. K using log function was created. The water depth, humidity in the underwater welding region, and arc stability are all elements that influence the fatigue behavior of underwater welds.

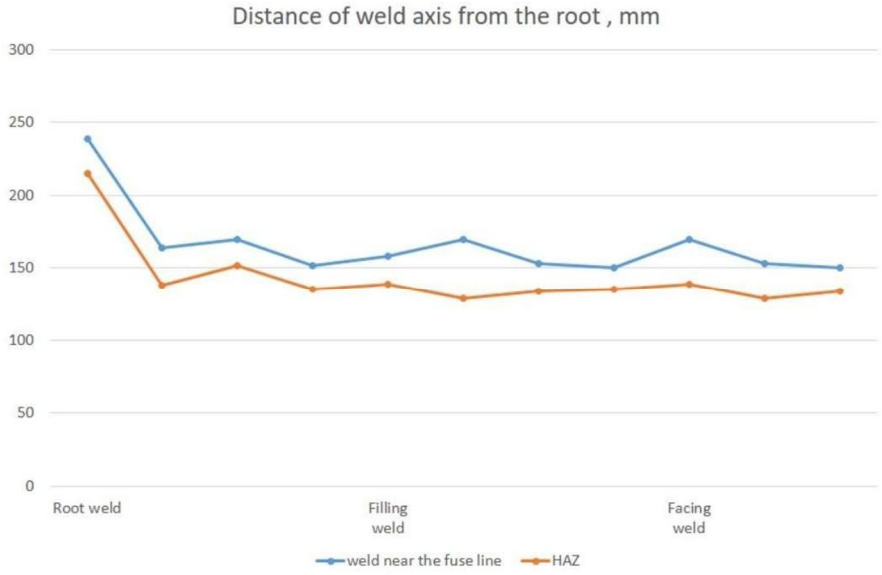

Fig.11 Distribution of hardness in the welded joint

A graph of hardness vs. distance along the weld axis from the root is examined, and the varied behavior of HAZ on different materials may be examined, revealing the weld's structural composition. In addition, maximum softening area, hardness decrease, and other parameters may be computed [69].

F. Mechanical Behavior of Materials

Apply sophisticated welding techniques, including as friction and laser welding, to better understand and optimize the behavior of materials and the welding process. Invented a novel welding process and investigated its potential for use in underwater welding. Cables and hoses used for electricity and gas supply typically restrict the robot's wrist mobility during the welding process [16]. The welding flame may be moved to each welding location and positioned perpendicular to the welding seam by the robot. It may approach locations in the work area from any angle and has one or more motion axes. This allows the robot to position the welding gun to weld components in a variety of ways.

In most cases, GMAW is the preferred method for robotic welding. Apart from minor radiation attenuation, the laser welding mechanisms for air and wet welding appear to be very similar. Although welds in holes deeper than 10 mm (0.4 inches) are porous, the majority of welds have mechanical strength in terms of strength and toughness. 12) Welded deposits on 2205 duplex stainless steel produced by the local cavity technique in air and under water revealed similar microstructure and characteristics [27].

The heat affected zones in all welds were extremely tiny, ranging in width from 0.2 to 0.6 mm, and increasing the welding heat input to 1.8 kJ/mm only marginally increased the width of the heat affected zone [37].

Tensile properties: Results indicated that underwater friction stir welding had a better joint efficiency than regular friction stir welding (60 percent and 55 percent respectively). There was a finding that friction welded joints performed better in terms of elongation generated, with 11.2 percent for the parent material vs. 4.56 percent for the welded junction [146].

1) *Macro and Microstructure:* When comparing the defect-free trapezoidal shape of the friction stir welding joint to the defect-free trapezoidal shape of the underwater friction stir welding joint, the defect-free trapezoidal shape is seen in friction stir welding but not in underwater friction stir welding. The grain size found in underwater friction stir welding is larger in SIR, smaller in MTR (Material Test Report), and finer in PIR [103].
2) *Micro Hardness:* During testing, it was discovered that the hardness level in underwater friction stir welding joints varies from 108 HV to 131 HV, whereas the hardness level in friction stir welding joints ranges from 108 HV to 120 HV. Lower hardness area [63] shows 90 to 94 HV.
3) *Fracture Surface Analysis:* Near the edge of tungsten metal arc welding, significant grain deformation occurs, resulting in local fractures with a reduced hardness.
4) *Finite Element Analysis:* In a friction stir welding joint, temperature is measured at the tool's leading and trailing edges in a lateral direction that is likewise asymmetrical.

The heat delivered to the preheat zone in underwater friction stir welding is given off by convective heat transfer through water. The warmup zone temperature was too low for underwater friction stir compared to friction stir. The temperature range was about 400 degrees Celsius at the FSW joint, which suggests a larger TMAZ area. Material takes on a plastic character at such high temperatures, but only a small portion of the ocean encounters such temperatures [41].

Ni-based weld metals are found to be completely austenitic in character, with columnar sub grain. Because of the fast-cooling rate and short retention period at high temperatures, grain boundary migration forms Type II boundaries in the austenite temperature range. The grain boundary thickens and liquefies in the microstructure of the base metal 304L. In the nickel-based weld, the columnar structure is visible.

The key components C, Fe, Cr, and Ni were studied, and it was discovered that the amount of Fe was substantially reduced, while Ni and Cr content steadily rose. When inspecting the interaction under a microscope. The Fe concentration of 304L/ER308 seldom changes, while the Cr level is negligible. As a result, the chemical composition distribution at the weld's contact between ferrite base metal and austenitic metal is more complex than at the uniform interface [63].

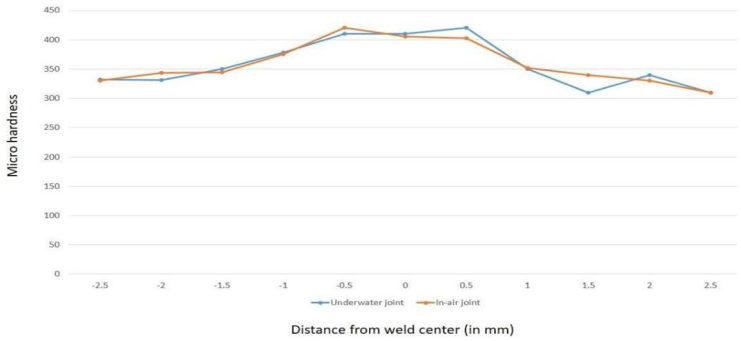

Fig. 12 micro hardness in underwater and in-air joints.

Underwater welding with moisture has a different melting point micro hardness curve than air welding. The nickel-based weld metal in the air has certain properties in common with water. Furthermore, the spacing between dendrites is affected by the cooling rate. On the 16Mn side, the measured limits of HAZ 304L and Type II HAZ are comparable to those observed underwater. The quantity of -ferrite present in the weld metal rises as the cooling rate increases in the microstructure of the DMW joint utilizing ER308 in the weld metal air [63].

The strength of the electric field, which has a direct effect on current and arc length, will increase as the water column rises due to a decrease in current arc diameter. It was also discovered that the volume of bubbles is related to the welding process's stability. Halogen gases were shown to be troublesome for the welding process during testing [63].

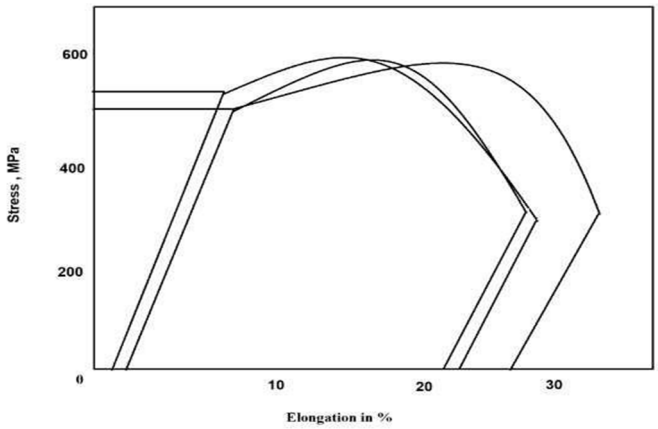

Fig. 13 Tensile stress curve vs. elongation

The SN curve technique, which represents the rotational bending load, is used to calculate fatigue resistance and fatigue life, and the threshold value may be seen of as a region where cracks do not form during growth. The link between the crack growth rate and the difference in working stress intensity is shown in the realm of Paris's law [10]. The second step before fracture occurs is the rate of crack growth. The last step of the propagation process occurs at a very quick pace in the graph's ultimate failure zone, so that the tension intensity propagation exceeds the value of critical stress intensity [8].

The hand wheel and the bottom plate are used for explosive welding. The explosive explosion accelerates the flying board to the speed VP, and then the speed VP collides with the substrate at a certain angle (called the collision angle). It is proportional to the angle of contact. The kinetic energy of the flight board is transformed into various kinds of energy during the collision, resulting in high pressure at the connection's interface, and therefore the weld seam is created owing to the massive pressure of the metal flow [33].

G. Droplet and Bubble Formation

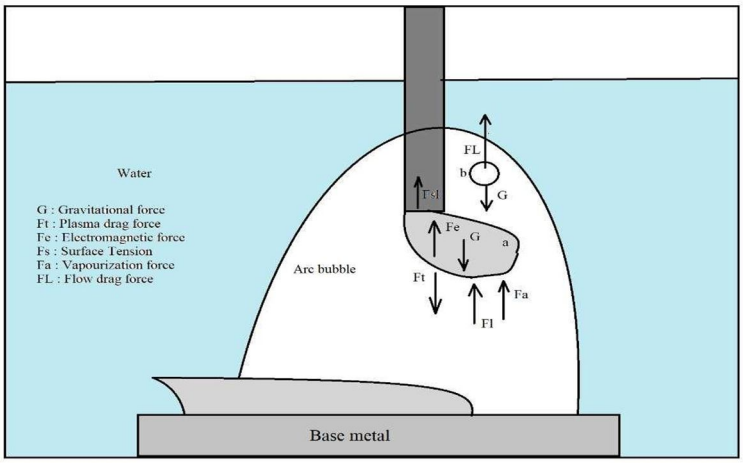

Fig. 14 Force acting on the droplet

It may be determined whether the bubble size rises or decreases based on the solution of this equation (bubble-water- (1 / R1 + 1 / R2)). The horizontal expansion of the bubble is thicker than the bubble growth along the z-axis or along the height, according to both experimental and numerical findings. The contraction phase 1 begins at the bottom. Due to the frequent expansion and contraction of arc bubbles, be careful not to introduce water into the arc [1]. Bubble development is divided into three stages: growth, soil compression, and separation. The microstructure of UFCAW welded joints has been discovered to be made up of three parts: eutectoid ferrite, granular bainite, and acicular ferrite. The austenite grain size rises, the eutectoid ferrite (PF) repaired by ferrite changes into the eutectoid ferrite (PF) of the original eutectoid ferrite, and the upper bainite BU) is decreased and replaced by granular bainite under the action of ultrasound.

The use of ultrasound has also been shown to enhance the ductility of the welded joint. It was also discovered that the split surface vanished when the upper sample of the underwater ultrasonic wet weld was destroyed. The two peaks with the greatest peaks raise the likelihood to 17.5 percent when evaluating the electrical signal from the welding process, confirming that the welding process in the two cases is more stable than in the other situations. As a result of the mixture's protective action, the speed is significantly slowed. The elongation and maximum tensile strength of submerged arc welding have also been observed to improve [7].

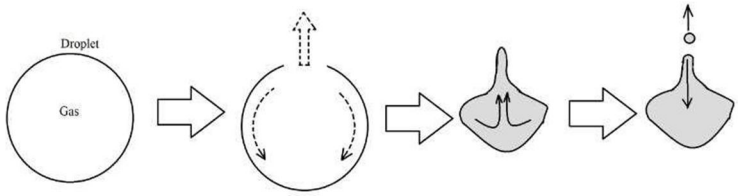

Fig. 15 Gas formed during welding process escaping water

The relative distance between the welding flame and the centerline of the molten pool rises as the welding speed increases, resulting in the molten pool lengthening. Furthermore, when welding speed increases, the weld seam improvement becomes extremely tiny. Because big bubbles are difficult to produce in the molten pool, the fluctuation in the molten pool is considerably decreased [9]. The content of diffusible hydrogen progressively increases as the welding speed increases. The diffusible hydrogen concentration in the weld metal is lower when the welding speed is less than 2.0 mm/s, which is a significant observation. Weld ability is present, and intricate interactions may be seen between each continuous layer of the weld and the preceding weld, as well as between the microscopically observable phases in the heat-affected zone. The base metal is determined by the austenite's cooling rate. The water around the arc boils and transforms into vapor bubbles during underwater wet welding. The arc bubble's growth has a substantial impact on the fall. The molten droplet penetrates the welding pool and turns it into a mist, which is rejected by the molten droplet due to the strong repulsive force. The LUADTC technique, as compared to standard wet welding, reduces average weld width and average weld reinforcement strength, and improves the metal [45].

The last observation is to enhance underwater welding efficiency. Reduce the number of flaws and inclusions in your welds. Almost all of the tests utilizing various metals, restrictions, and parameters showed improvements in mechanical and microstructural characteristics. Some of these modifications have occurred. Is excellent, but the remainder must be managed so that the weld is successful. To avoid unneeded modifications, this must be done in a tightly controlled setting [15].

H. Miscellaneous

The pictures of arc bubble dynamic behavior in underwater arc welding at various times are exhibited, and it aids the material's underwater weld quality. It also assures the quality and stability of the weld zone. To produce but joints, different feed rates and travel speeds are utilized, and the effect of the speed determines the breadth of the weld. A graph of weld width vs. travel speed is created, followed by tensile and impact toughness calculations and drawings, all of which aid improve weld quality. The weld rotational & water rotational dynamical effects in the weld region are improved by plotting rotational speed vs. tensile strength.

The weld in the rotating welding technique is also affected by the metal composition [45]. The solubility of hydrogen at different temperatures can impact the weld, since it can cause large bubbles to develop and the welded structure to collapse, according to a microstructural pool x-ray. The weld rotational & water rotational dynamical impacts in the weld zone region are improved by plotting rotational speed vs. tensile strength. The composition of the metal has an impact as well. Weld using a rotating welding technique the solubility of hydrogen at different temperatures can impact the weld, since it can cause large bubbles to develop and the welded structure to collapse [122]. Microstructural pool x-rays were drawn and observations were made.

ISSN: 2321-9653; IC Value: 45.98; SJ Impact Factor: 7.429
Volume 9 Issue XI Nov 2021- Available at www.ijraset.com

On various materials, the tool rotation velocity (rpm) and transverse velocity (mm/min) are estimated to aid in the strength and tensile computation of the weld.

In addition, graphs of thickness and rotation speeds have been created. The welding parameters such as wire feeding rate and arc voltage welding current fluctuation with respect to time were plotted using a high-speed camera. The microstructural characteristics of the weld aid in the appropriate dynamical concept [6].

Positive pressure welding is done in a sealed chamber close to the structure that has to be welded. At the main pressure, the chamber is filled with gas (typically helium with 0.5 bar oxygen). The habitat is enclosed in pipes and filled with a breathable helium/oxygen combination. At or slightly over the appropriate welding pressure. Despite the fact that the range of this area is smaller than 0.5 mm, the hardness value is close to 600 Hk (100 g).

Because the greater the 3/16 inch, the more heat accumulated, HAZ hardening in underwater welding will not go out of hand. The less hardness induced by the electrode, the better. The weld form in underwater and air welding is found to be fairly comparable [86] when the welding current and velocity are the same.

V. CONCLUSION

A. Wet welding and dry welding are the two main forms of underwater welding. Underwater wet welding (UWW) provides a number of advantages, including simpler equipment, more mobility, reduced preparation time, and lower costs. Underwater dry welding, on the other hand, is costly, requires a complex equipment, and limits the diver's movement. Dry welding can result in a high-quality weld. Wet welding, on the other hand, is ideal for maintenance and repair work since it is far less expensive than dry welding.

B. The cooling system is good since the welding is done under water; thus, grain coarsening and precipitation are significantly minimized, resulting in higher joint strength. The weld's mechanical and microstructural characteristics are improved.

C. The type of weld to be used is influenced by the depth of the water, the waves in the water, and the temperature of the water. They are extremely important in defining the weld characteristics. Porosity, brittleness, crack propagation, and bubble formation all increase as depth increases.

D. Welding speed and angle are both important factors in determining weld quality and flaws. Welding at a slow pace can result in bulges, while welding at a fast speed might result in pits, lowering the quality of the weld. The number of passes in the superheated section of the welded connection is inversely related to the strength, according to experimental data.

E. Underwater welding may be done both in water and in a dry environment using a specially constructed pressure shell.

VI. FUTURE SCOPE AND RESEARCH DIRECTION:

There are numerous unsolved difficulties in the field of marine and offshore welding, which need further study and knowledge. This article provides a basic overview of underwater welding, including the principals involved, as well as the benefits and drawbacks of various forms of underwater welding. The current traditional procedures are discussed, as well as some best practices. One of the most effective welding processes is underwater friction stir welding, which allows you to fuse a variety of materials while maintaining good mechanical and tensile strength.

Water acts as a cooling medium, aiding the microstructural development of the weld, making this welding process more effective than its onshore counterpart. The use of a twin gas nozzle in submerged arc welding to form an air cavity above the weld zone, which separates the weld zone from the impact of water, is another helpful approach. Stick welding using polymer coated electrodes has been a huge success; the polymer serves as a flux and protects the weldment.

The polymers can be further investigated in order to expand the possibilities for underwater welding. The addition of organic resin aided welding to the research is a bonus. These variables can be investigated further. All other welding processes, like the ones described above, have demonstrated outstanding performance throughout time and can be further investigated in order to achieve the aim of flawless underwater welding. Finally, with the advancement of technology, further research is recommended.

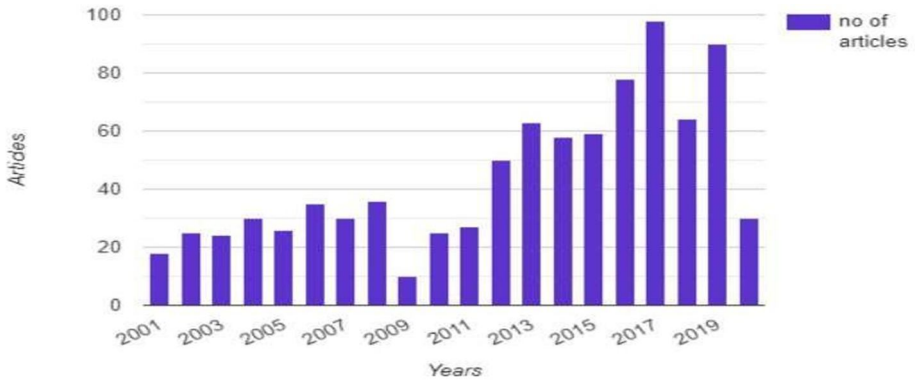

Fig. 16 Underwater welding research work over the years

Furthermore, in recent years, research in the field of underwater welding has declined substantially. To achieve the aim of flawless welding, more effort must be done.

REFERENCES

[1] Zhao B, Chen J, Wu C, Shi L. Numerical simulation of bubble and arc dynamics during underwater wet flux-cored arc welding. J Manuf Process. 2020;59:167-185. doi:10.1016/j.jmapro.2020.09.054
[2] Liu D, Li HL, Yan YT, Guo N, Song XG, Feng JC. Effects of processing parameters on arc stability and cutting quality in underwater wet flux-cored arc cutting at shallow water. J Manuf Process. 2018;33:24-34. doi:10.1016/j.jmapro.2018.04.021
[3] Xing C, Jia C, Han Y, Dong S, Yang J, Wu C. Numerical Analysis of the Metal Transfer and Welding Arc Behaviors in Underwater Flux-cored Arc Welding. Int J Heat Mass Transf. 2020;153. doi:10.1016/j.ijheatmasstransfer.2020.119570
[4] Guo N, Wang M, Du Y, Guo W, Feng J. Metal transfer in underwater flux-cored wire wet welding at shallow water depth. Mater Lett. 2015;144:90-92. doi:10.1016/j.matlet.2015.01.033
[5] Amaral EC, Moreno-Uribe AM, Bracarense AQ. Effects of PTFE on operational characteristics and diffusible H and O contents of weld metal in underwater wet welding. J Manuf Process. 2021;61:270-279. doi:10.1016/j.jmapro.2020.11.018
[6] Guo N, Xu C, Guo W, Du Y, Feng J. Characterization of spatter in underwater wet welding by X-ray transmission method. Mater Des. 2015;85:156-161. doi:10.1016/j.matdes.2015.06.152
[7] Feng J, Wang J, Sun Q, Zhao H, Wu L, Xu P. Investigation on dynamic behaviors of bubble evolution in underwater wet flux-cored arc welding. J Manuf Process. 2017;28:156-167. doi:10.1016/j.jmapro.2017.06.003
[8] Igwemezie V, Dirisu P, Mehmanparast A. Critical assessment of the fatigue crack growth rate sensitivity to material microstructure in ferrite-pearlite steels in air and marine environment. Mater Sci Eng A. 2019;754:750-765. doi:10.1016/j.msea.2019.03.093
[9] Wang J, Sun Q, Pan Z, Yang J, Feng J. Effects of welding speed on bubble dynamics and process stability in mechanical constraint-assisted underwater wet welding of steel sheets. J Mater Process Technol. 2019;264:389-401. doi:10.1016/j.jmatprotec.2018.09.022
[10] Wang Y, Yuan L, Zhang S, et al. The influence of combined gradient structure with residual stress on crack-growth behavior in medium carbon steel. Eng Fract Mech. 2019;209:369-381. doi:10.1016/j.engfracmech.2019.01.037
[11] Xu C, Guo N, Zhang X, Chen H, Fu Y, Zhou L. Internal characteristic of droplet and its influence on the underwater wet welding process stability. J Mater Process Technol. 2020;280. doi:10.1016/j.jmatprotec.2020.116593
[12] Zhang Y, Jia C, Zhao B, Hu J, Wu C. Heat input and metal transfer influences on the weld geometry and microstructure during underwater wet FCAW. J Mater Process Technol. 2016;238:373-382. doi:10.1016/j.jmatprotec.2016.07.024
[13] Wang J, Sun Q, Zhang S, Wang C, Wu L, Feng J. Characterization of the underwater welding arc bubble through a visual sensing method. J Mater Process Technol. 2018;251:95-108. doi:10.1016/j.jmatprotec.2017.08.019
[14] Yin Y, Yang X, Cui L, Wang F, Li S. Material flow influence on the weld formation and mechanical performance in underwater friction taper plug welds for pipeline steel. Mater Des. 2015;88:990-998. doi:10.1016/j.matdes.2015.09.123
[15] Yang Q, Han Y, Jia C, Wu J, Dong S, Wu C. Impeding effect of bubbles on metal transfer in underwater wet FCAW. J Manuf Process. 2019;45:682-689. doi:10.1016/j.jmapro.2019.08.013
[16] Sun QJ, Cheng WQ, Liu YB, Wang JF, Cai CW, Feng JC. Microstructure and mechanical properties of ultrasonic assisted underwater wet welding joints. Mater Des. 2016;103:63-70. doi:10.1016/j.matdes.2016.04.019
[17] Świerczyńska A, Fydrych D, Rogalski G. Diffusible hydrogen management in underwater wet self-shielded flux cored arc welding. Int J Hydrogen Energy. 2017;42(38):24532-24540. doi:10.1016/j.ijhydene.2017.07.225
[18] Muhayat N, Matien YA, Sukanto H, Saputro YCN, Triyono. Fatigue life of underwater wet welded low carbon steel SS400. Heliyon. 2020;6(2). doi:10.1016/j.heliyon.2020.e03366
[19] Gao W, Wang D, Cheng F, Deng C, Liu Y, Xu W. Enhancement of the fatigue strength of underwater wet welds by grinding and ultrasonic impact treatment. J Mater Process Technol. 2015;223:305-312. doi:10.1016/j.jmatprotec.2015.04.013
[20] Hu Y, Shi Y, Sun K, Shen X, Wang Z. Microstructure and mechanical properties of underwater hyperbaric FCA-welded duplex stainless steel joints. J Mater Process Technol. 2018;261:31-38. doi:10.1016/j.jmatprotec.2018.05.027
[21] Heirani F, Abbasi A, Ardestani M. Effects of processing parameters on microstructure and mechanical behaviors of underwater friction stir welding of Al5083 alloy. J Manuf Process. 2017;25:77-84. doi:10.1016/j.jmapro.2016.11.002

[22] Guo N, Liu D, Guo W, Li H, Feng J. Effect of Ni on microstructure and mechanical properties of underwater wet welding joint. Mater Des. 2015;77:25-31. doi:10.1016/j.matdes.2015.04.007
[23] Gao W, Wang D, Cheng F, Di X, Deng C, Xu W. Microstructural and mechanical performance of underwater wet welded S355 steel. J Mater Process Technol. 2016;238:333-340. doi:10.1016/j.jmatprotec.2016.07.039
[24] Guo N, Du Y, Feng J, Guo W, Deng Z. Study of underwater wet welding stability using an X- ray transmission method. J Mater Process Technol. 2015;225:133-138. doi:10.1016/j.jmatprotec.2015.06.003
[25] Chen H, Guo N, Xu K, Xu C, Zhou L, Wang G. In-situ observations of melt degassing and hydrogen removal enhanced by ultrasonics in underwater wet welding. Mater Des. 2020;188. doi:10.1016/j.matdes.2020.108482
[26] Di X, Ji S, Cheng F, Wang D, Cao J. Effect of cooling rate on microstructure, inclusions and mechanical properties of weld metal in simulated local dry underwater welding. Mater Des. 2015;88:505-513. doi:10.1016/j.matdes.2015.09.025
[27] Cui L, Yang X, Wang D, Hou X, Cao J, Xu W. Friction taper plug welding for S355 steel in underwater wet conditions: Welding performance, microstructures and mechanical properties. Mater Sci Eng A. 2014;611:15-28. doi:10.1016/j.msea.2014.04.087
[28] Chen H, Guo N, Liu C, Zhang X, Xu C, Wang G. Insight into hydrostatic pressure effects on diffusible hydrogen content in wet welding joints using in-situ X-ray imaging method. Int J Hydrogen Energy. 2020;45(16):10219-10226. doi:10.1016/j.ijhydene.2020.01.195
[29] Chen H, Guo N, Shi X, Du Y, Feng J, Wang G. Effect of water flow on the arc stability and metal transfer in underwater flux-cored wet welding. J Manuf Process. 2018;31:103-115. doi:10.1016/j.jmapro.2017.11.010
[30] Łabanowski J. Development of under-water welding techniques. Weld Int. 2011;25(12):933- 937. doi:10.1080/09507116.2010.540847
[31] Rodriguez-Sanchez JE, Perez-Guerrero F, Liu S, Rodriguez-Castellanos A, Albiter-Hernandez A. Underwater repair of fatigue cracks by gas tungsten arc welding process. Fatigue Fract Eng Mater Struct. 2014;37(6):637-644. doi:10.1111/ffe.12146
[32] Putri EDWS, Surojo E, Budiana EP, Triyono. Current research and recommended development on fatigue behavior of underwater welded steel. In: Procedia Structural Integrity. Vol 27. Elsevier B.V.; 2020:54-61. doi:10.1016/j.prostr.2020.07.008
[33] Arias AR, Bracarense AQ. Fatigue crack growth rate in underwater wet welds: out of water evaluation. Weld Int. 2017;31(5):348-353. doi:10.1080/09507116.2016.1218607
[34] Oikonomou AG, Aggidis GA. Determination of optimum welding parameters for the welding execution of steels used in underwater marine systems (including the submerged parts of Wave Energy Converters). In: Materials Today: Proceedings. Vol 18. Elsevier Ltd; 2019:455-461. doi:10.1016/j.matpr.2019.06.211
[35] Oikonomou AG, Aggidis GA. Determination of the corrosion resistance of the welded steels used in underwater marine systems (including the submerged parts of wave energy converters). Mater Today Proc. 2020;44:5048-5053. doi:10.1016/j.matpr.2020.06.393
[36] Li HL, Liu D, Yan YT, Guo N, Liu YB, Feng JC. Effects of heat input on arc stability and weld quality in underwater wet flux-cored arc welding of E40 steel. J Manuf Process. 2018;31:833- 843. doi:10.1016/j.jmapro.2018.01.013
[37] Prabowo AR, Ubaidillah, Imaduddin F. Editorial: Integrity of mechanical structure and material. Procedia Struct Integr. 2020;27:1-5. doi:10.1016/j.prostr.2020.07.001
[38] Baillie P, Campbell SW, Galloway AM, Cater SR, McPherson NA. Friction stir welding of 6mm thick carbon steel underwater and in air. Sci Technol Weld Join. 2015;20(7):585-593. doi:10.1179/1362171815Y.0000000042
[39] Doyen J, Castellucci P, Colchen D. Fatigue strength of joints made in hyperbaric and wet underwater welding. Weld Int. 1992;6(4):287-291. doi:10.1080/09507119209548186
[40] Bae DM, Prabowo AR, Cao B, Zakki AF, Haryadi GD. Study on collision between two ships using selected parameters in collision simulation. J Mar Sci Appl. 2016;15(1):63-72. doi:10.1007/s11804-016-1341-2
[41] Liu HJ, Zhang HJ, Huang YX, Yu L. Mechanical properties of underwater friction stir welded 2219 aluminum alloy. Trans Nonferrous Met Soc China (English Ed. 2010;20(8):1387-1391. doi:10.1016/S1003-6326(09)60309-5
[42] Fydrych D, Łabanowski J, Rogalski G. Weldability of high strength steels in wet welding conditions. Polish Marit Res. 2013;20(2):67-73. doi:10.2478/pomr-2013-0018
[43] Nixon JH. Underwater welding technology. In: Underwater Repair Technology. Elsevier; 2000:25-37. doi:10.1533/9781855738867.25
[44] Bae DM, Prabowo AR, Cao B, Sohn JM, Zakki AF, Wang Q. Numerical simulation for the collision between side structure and level ice in event of side impact scenario. Lat Am J Solids Struct. 2016;13(16):2691-2704. doi:10.1590/1679-78252975
[45] Chen H, Guo N, Shi X, Du Y, Feng J, Wang G. Effect of hydrostatic pressure on protective bubble characteristic and weld quality in underwater flux-cored wire wet welding. J Mater Process Technol. 2018;259:159-168. doi:10.1016/j.jmatprotec.2018.04.037
[46] Tan YB, Wang XM, Ma M, et al. A study on microstructure and mechanical properties of AA 3003 aluminum alloy joints by underwater friction stir welding. Mater Charact. 2017;127:41- 52. doi:10.1016/j.matchar.2017.01.039
[47] Zhang HJ, Liu HJ, Yu L. Effect of water cooling on the performances of friction stir welding heat-affected zone. J Mater Eng Perform. 2012;21(7):1182-1187. doi:10.1007/s11665-011- 0060-8
[48] Chen H, Zhang Y, Dai Y, Min C, Zhu S, Yuan X. Facilitated tip-enhanced Raman scattering by focused gap-plasmon hybridization. Photonics Res. 2020;8(2):103. doi:10.1364/prj.8.000103
[49] Bahatmaka A, Kim DJ, Prabowo AR. Numerical investigation against laboratory experiment: An overview of damage and wind loads on structural design. In: Procedia Structural Integrity. Vol 27. Elsevier B.V.; 2020:6-13. doi:10.1016/j.prostr.2020.07.002
[50] Prasetya LW, Prabowo AR, Ubaidillah, Nordin NAB. Crashworthiness analysis of attenuator structure based on recycled waste can subjected to impact loading: Part i - Absorption performance. In: Procedia Structural Integrity. Vol 27. Elsevier B.V.; 2020:125-131. doi:10.1016/j.prostr.2020.07.017
[51] Recent Developments on Underwater Welding of Metallic Material - ScienceDirect. Accessed May 6, 2021. https://www.sciencedirect.com/science/article/pii/S245232162030473X
[52] Ćwiek J. Hydrogen assisted cracking of high-strength weldable steels in sea-water. J Mater Process Technol. 2005;164-165:1007-1013. doi:10.1016/j.jmatprotec.2005.02.083

[53] Surojo E, Putri EDWS, Budiana EP, Triyono. Recent developments on underwater welding of metallic material. In: Procedia Structural Integrity. Vol 27. Elsevier B.V.; 2020:14-21. doi:10.1016/j.prostr.2020.07.003
[54] Menezes PHR, Pessoa ECP, Bracarense AQ. Comparison of underwater wet welding performed with silicate and polymer agglomerated electrodes. J Mater Process Technol. 2019;266:63-72. doi:10.1016/j.jmatprotec.2018.10.019
[55] Vaz CT, Bracarense AQ, Felizardo I, Pereira Pessoa EC. Impermeable low hydrogen covered electrodes: Weld metal, slag, and fumes evaluation. J Mater Res Technol. 2012;1(2):64-70. doi:10.1016/S2238-7854(12)70012-1
[56] Li W, Zhao J, Wang Y, et al. Research on underwater flux cored arc cutting mechanism based on simulation of kerf formation. J Manuf Process. 2019;40:169-177. doi:10.1016/j.jmapro.2019.03.010
[57] Wang J, Sun Q, Jiang Y, Zhang T, Ma J, Feng J. Analysis and improvement of underwater wet welding process stability with static mechanical constraint support. J Manuf Process. 2018;34:238-250. doi:10.1016/j.jmapro.2018.06.007
[58] Ramírez Luna LE, Bracarense AQ, Pessoa ECP, Costa PS, Altamirano Guerrero G, Salas Reyes AE. Effect of the welding angle on the porosity of underwater wet welds performed in overhead position at different simulated depths. J Mater Process Technol. 2021;294. doi:10.1016/j.jmatprotec.2021.117114
[59] Klett J, Mattos IBF, Maier HJ, e Silva RHG, Hassel T. Control of the diffusible hydrogen content in different steel phases through the targeted use of different welding consumables in underwater wet welding. Mater Corros. 2021;72(3):504-516. doi:10.1002/maco.202011963
[60] Tomków J. Weldability of underwater wet-welded HSLA steel: Effects of electrode hydrophobic coatings. Materials (Basel). 2021;14(6). doi:10.3390/ma14061364
[61] Xu C, Guo N, Zhang X, Jiang H, Tan Y, Zhou L. Influence of welding speed on weld pool dynamics and welding quality in underwater wet FCAW. J Manuf Process. 2020;55:381-388. doi:10.1016/j.jmapro.2020.03.046
[62] Fu Y, Guo N, Zhou L, Cheng Q, Feng J. Underwater wire-feed laser deposition of the Ti–6Al– 4V titanium alloy. Mater Des. 2020;186. doi:10.1016/j.matdes.2019.108284
[63] Wei P, Li H, Liu J, et al. The effect of water environment on microstructural characteristics, compositional heterogeneity and microhardness distribution of 16Mn/304L dissimilar welded joints. J Manuf Process. 2020;56:417-427. doi:10.1016/j.jmapro.2020.05.006
[64] Fu Y, Guo N, Du Y, Chen H, Xu C, Feng J. Effect of metal transfer mode on spatter and arc stability in underwater flux-cored wire wet welding. J Manuf Process. 2018;35:161-168. doi:10.1016/j.jmapro.2018.07.027
[65] Çolak Z, Ayan Y, Kahraman N. Weld morphology and mechanical performance of marine structural steel welded underwater in a real marine environment. Int J Adv Manuf Technol. 2020;109(1-2):491-501. doi:10.1007/s00170-020-05679-y
[66] Wang T, Yu B, Han K, et al. Effect of heat input on microstructure and mechanical properties of Ti/Cu66V34/Cu joints by electron beam welding. J Manuf Process. 2019;45:147-153. doi:10.1016/j.jmapro.2019.07.005
[67] Zhang X, Guo N, Xu C, Du Y, Chen B, Feng J. Influence of CaF2 on microstructural characteristics and mechanical properties of 304 stainless steel underwater wet welding using flux-cored wire. J Manuf Process. 2019;45:138-146. doi:10.1016/j.jmapro.2019.07.003
[68] Zhang S, Li H, Jiang Z, et al. Influence of N on precipitation behavior, associated corrosion and mechanical properties of super austenitic stainless steel S32654. J Mater Sci Technol. 2020;42:143-155. doi:10.1016/j.jmst.2019.10.011
[69] Gao J, Tan J, Jiao M, Wu X, Tang L, Huang Y. Role of welding residual strain and ductility dip cracking on corrosion fatigue behavior of Alloy 52/52M dissimilar metal weld in borated and lithiated high-temperature water. J Mater Sci Technol. 2020;42:163-174. doi:10.1016/j.jmst.2019.10.012
[70] Wu J, Jin L, Dong J, Wang F, Dong S. The texture and its optimization in magnesium alloy. J Mater Sci Technol. 2020;42:175-189. doi:10.1016/j.jmst.2019.10.010
[71] Drobny JG. Processing Methods Applicable to Thermoplastic Elastomers. In: Handbook of Thermoplastic Elastomers. Elsevier; 2014:33-173. doi:10.1016/b978-0-323-22136-8.00004-1
[72] Wang C, Cheng L, Liu Y, Zhu C. Ultrasonic flexible bulging process of spherical caps array as surface texturing using aluminum alloy 5052 ultra-thin sheet. J Mater Process Technol. 2020;284. doi:10.1016/j.jmatprotec.2020.116725
[73] Lima CRC, Belém MJX, Fals HDC, Rovere CAD. Wear and corrosion performance of Stellite 6® coatings applied by HVOF spraying and GTAW hotwire cladding. J Mater Process Technol. 2020;284. doi:10.1016/j.jmatprotec.2020.116734
[74] Dong S, Han Y, Jia C, et al. Organic adhesive assisted underwater submerged-arc welding. J Mater Process Technol. 2020;284:116739. doi:10.1016/j.jmatprotec.2020.116739
[75] Organic adhesive assisted underwater submerged-arc welding - ScienceDirect. Accessed May 6, 2021. https://www.sciencedirect.com/science/article/abs/pii/S0924013620301539
[76] Banik S Das, Kumar S, Singh PK, Bhattacharya S, Mahapatra MM. Distortion and residual stresses in thick plate weld joint of austenitic stainless steel: Experiments and analysis. J Mater Process Technol. 2021;289. doi:10.1016/j.jmatprotec.2020.116944
[77] Fu Y, Guo N, Zhou C, Wang G, Feng J. Investigation on in-situ laser cladding coating of the 304 stainless steel in water environment. J Mater Process Technol. 2021;289:116949. doi:10.1016/j.jmatprotec.2020.116949
[78] HINO T, TAMURA M, TANAKA Y, et al. Development of Underwater Laser Cladding and Underwater Laser Seal Welding Techniques for Reactor Components. J Power Energy Syst. 2009;3(1):51-59. doi:10.1299/jpes.3.51
[79] Yoda M, Tamura M, Fukuda T, et al. Underwater laser beam welding for nuclear reactors. In: International Conference on Nuclear Engineering, Proceedings, ICONE. Vol 1. American Society of Mechanical Engineers (ASME); 2012:191-195. doi:10.1115/ICONE20- POWER2012-54836
[80] Çam G, İpekoğlu G. Recent developments in joining of aluminum alloys. Int J Adv Manuf Technol. 2017;91(5-8):1851-1866. doi:10.1007/s00170-016-9861-0
[81] SANO Y, MUKAI N, MAKINO Y, et al. Enhancement of Surface Properties of Metal Materials by Underwater Laser Processing. Rev Laser Eng. 2008;36(APLS):1195-1198. doi:10.2184/lsj.36.1195
[82] Shannon GJ, McNaught W, Deans WF, Watson J. High power laser welding in hyperbaric gas and water environments. J Laser Appl. 1997;9(3):129-136. doi:10.2351/1.4745452
[83] Fu Y, Guo N, Cheng Q, Zhang D, Feng J. Underwater laser welding for 304 stainless steel with filler wire. J Mater Res Technol. 2020;9(6):15648-15661. doi:10.1016/j.jmrt.2020.11.029

[84] Tian J, Fu X, Shao X, Jiang L, Li J, Kan Q. Damage-coupled ratcheting behaviors of SA508 Gr.3 steel at room and elevated temperatures: Experiments and simulations. Int J Damage Mech. 2020;29(9):1379-1396. doi:10.1177/1056789520930406
[85] Mohanty S, Majumdar S, Natesan K. Steam generator tube rupture simulation using extended finite element method. Nucl Eng Des. 2016;305:697-705. doi:10.1016/j.nucengdes.2016.06.031
[86] Mohanty S, Soppet WK, Majumdar S, Natesan K. Chaboche-based cyclic material hardening models for 316 SS–316 SS weld under in-air and pressurized water reactor water conditions.mNucl Eng Des. 2016;305:524-530. doi:10.1016/j.nucengdes.2016.05.031
[87] Gao J, Zhang Z, Tan J, et al. Differences of corrosion fatigue behaviors among 316LN base metal, 316LN heat-affected zone and 308L weld metal in a safe-end weld joint in borated and lithiated high-temperature water. Int J Fatigue. 2021;148. doi:10.1016/j.ijfatigue.2021.106223
[88] He P, Wang Z, Ye Z, Yang L, Gou F, Zhang K. Evolution of liquid lithium corrosion behavior for CLF-1 steels induced by high-flux helium irradiation. J Nucl Mater. 2020;539. doi:10.1016/j.jnucmat.2020.152269
[89] Jiang S, Shen J, Nagasaka T, et al. Interfacial characterization of dissimilar-metals bonding between vanadium alloy and Hastelloy X alloy by explosive welding. J Nucl Mater. 2020;539. doi:10.1016/j.jnucmat.2020.152322
[90] Gao J, Zhang Z, Tan J, Wu X, Han EH, Ke W. Environmentally assisted fatigue behavior of 308L weld metal in borated and lithiated high-temperature water. J Nucl Mater. 2020;539:152365. doi:10.1016/j.jnucmat.2020.152365
[91] Gao J, Zhang Z, Tan J, et al. Differences of corrosion fatigue behaviors among 316LN base metal, 316LN heat-affected zone and 308L weld metal in a safe-end weld joint in borated and lithiated high-temperature water. Int J Fatigue. 2021;148:106223. doi:10.1016/j.ijfatigue.2021.106223
[92] Vikas KSR, Raghu Ram N, Sai Charan B, Indrakanti SS. Hot pressing of copper and copper- based composites: Microstructure and suitability as electrodes for electric discharge machining. Mater Today Proc. 2021;41:1001-1007. doi:10.1016/j.matpr.2020.06.069
[93] Satyanarayana MVN., Reddy P, Kumar A. Preparation of bulk-area stir zone in aluminium 6061 alloy via cryogenic friction stir processing. Mater Today Proc. 2021;41:987-990. doi:10.1016/j.matpr.2020.05.730
[94] Microstructures and mechanical properties of friction stir spot welded Al 6061 alloy lap joint welded in air and water - ScienceDirect. Accessed May 6, 2021. https://www.sciencedirect.com/science/article/pii/S2214785320345120
[95] George K, Biswal M, Mohanty S, Nayak SK, Panda BP. Nanosilica filled EPDM/Kevlar fiber hybrid nanocomposites: Mechanical and thermal properties. Mater Today Proc. 2021;41:983- 986. doi:10.1016/j.matpr.2020.02.817
[96] Satputaley SS, Waware Y, Ksheersagar K, Jichkar Y, Khonde K. Experimental investigation on effect of TIG welding process on chromoly 4130 and aluminum 7075-T6. Mater Today Proc. 2021;41:991-994. doi:10.1016/j.matpr.2020.05.733
[97] Shekhawat RS, Nadakuduru VN, Nagumothu KB. Microstructures and mechanical properties of friction stir spot welded Al 6061 alloy lap joint welded in air and water. Mater Today Proc. 2021;41:995-1000. doi:10.1016/j.matpr.2020.06.065
[98] Luo M, Hu R, Li Q, Huang A, Pang S. Physical understanding of keyhole and weld pool dynamics in laser welding under different water pressures. Int J Heat Mass Transf. 2019;137:328-336. doi:10.1016/j.ijheatmasstransfer.2019.03.129
[99] Sree Sabari S, Malarvizhi S, Balasubramanian V, Madusudhan Reddy G. Experimental and numerical investigation on under-water friction stir welding of armour grade AA2519-T87 aluminium alloy. Def Technol. 2016;12(4):324-333. doi:10.1016/j.dt.2016.02.003
[100] Godwin Barnabas S, Rajakarunakaran S, Satish Pandian G, Muhamed Ismail Buhari A, Muralidharan V. Review on enhancement techniques necessary for the improvement of underwater welding. Mater Today Proc. Published online April 15, 2020. doi:10.1016/j.matpr.2020.03.725
[101] Papahn H, Bahemmat P, Haghpanahi M, Sommitsch C. Study on governing parameters of thermal history during underwater friction stir welding. Int J Adv Manuf Technol. 2015;78(5- 8):1101-1111. doi:10.1007/s00170-014-6615-8
[102] Liang H, Yan K, Wang Q, Zhao Y, Liu C, Zhang H. Improvement in Joint Strength of Spray- Deposited Al-Zn-Mg-Cu Alloy in Underwater Friction Stir Welding by Altered Temperature of Cooling Water. J Mater Eng Perform. 2016;25(12):5486-5493. doi:10.1007/s11665-016-2383- y
[103] Zhang HJ, Liu HJ, Yu L. Microstructural evolution and its effect on mechanical performance of joint in underwater friction stir welded 2219-T6 aluminium alloy. Sci Technol Weld Join. 2011;16(5):459-464. doi:10.1179/1362171811Y.0000000024
[104] Zhang H, Liu H. Characteristics and Formation Mechanisms of Welding Defects in Underwater Friction Stir Welded Aluminum Alloy. Metallogr Microstruct Anal. 2012;1(6):269-281. doi:10.1007/s13632-012-0038-4
[105] Eyvazian A, Hamouda A, Tarlochan F, Derazkola HA, Khodabakhshi F. Simulation and experimental study of underwater dissimilar friction-stir welding between aluminium and steel. J Mater Res Technol. 2020;9(3):3767-3781. doi:10.1016/j.jmrt.2020.02.003
[106] Liu HJ, Zhang HJ, Yu L. Homogeneity of mechanical properties of underwater friction stir welded 2219-T6 aluminum alloy. In: Journal of Materials Engineering and Performance. Vol 20. ; 2011:1419-1422. doi:10.1007/s11665-010-9787-x
[107] Derazkola HA, Khodabakhshi F. Underwater submerged dissimilar friction-stir welding of AA5083 aluminum alloy and A441 AISI steel. Int J Adv Manuf Technol. 2019;102(9-12):4383- 4395. doi:10.1007/s00170-019-03544-1
[108] Kawahito Y, Wang H. In-situ observation of gap filling in laser butt welding. Scr Mater. 2018;154:73-77. doi:10.1016/j.scriptamat.2018.05.033
[109] Sudnik W, Radaj D, Breitschwerdt S, Erofeew W. Numerical simulation of weld pool geometry in laser beam welding. J Phys D Appl Phys. 2000;33(6):662-671. doi:10.1088/0022- 3727/33/6/312
[110] Wang X, Wu C, Chen M. Numerical simulation of weld pool keyholing process in stationary plasma arc welding. Jinshu Xuebao/Acta Metall Sin. 2010;46(8):984-990. doi:10.3724/SP.J.1037.2010.00021
[111] David SA, DebRoy T. Current issues and problems in welding science. Science (80-). 1992;257(5069):497-502. doi:10.1126/science.257.5069.497
[112] Bae KY, Lee TH, Ahn KC. An optical sensing system for seam tracking and weld pool control in gas metal arc welding of steel pipe. J Mater Process Technol. 2002;120(1-3):458-465. doi:10.1016/S0924-0136(01)01216-X
[113] Yamada T, Shobu T, Nishimura A, Yonemoto Y, Yamashita S, Muramatsu T. In-situ X-ray observation of molten pool depth during laser micro welding. J Laser Micro Nanoeng. 2012;7(3):244-248. doi:10.2961/jlmn.2012.03.0002
[114] Leung CLA, Marussi S, Atwood RC, Towrie M, Withers PJ, Lee PD. In situ X-ray imaging of defect and molten pool dynamics in laser additive manufacturing. Nat Commun. 2018;9(1). doi:10.1038/s41467-018-03734-7
[115] Debroy T, David SA. Physical processes in fusion welding. Rev Mod Phys. 1995;67(1):85-112. doi:10.1103/RevModPhys.67.85

[116] Wang Y, Tsai HL. Effects of surface active elements on weld pool fluid flow and weld penetration in gas metal arc welding. Metall Mater Trans B Process Metall Mater Process Sci. 2001;32(3):501-515. doi:10.1007/s11663-001-0035-5
[117] Zhang YM, Song HS, Saeed G. Observation of a dynamic specular weld pool surface. In: Measurement Science and Technology. Vol 17. Institute of Physics Publishing; 2006. doi:10.1088/0957-0233/17/6/L02
[118] Zhao B, Chen J, Jia C, Wu C. Numerical analysis of molten pool behavior during underwater wet FCAW process. J Manuf Process. 2018;32:538-552. doi:10.1016/j.jmapro.2018.03.020
[119] Aucott L, Wen SW, Dong H. The role of Ti carbonitride precipitates on fusion zone strength- toughness in submerged arc welded linepipe joints. Mater Sci Eng A. 2015;622:194-203. doi:10.1016/j.msea.2014.10.057
[120] Guo N, Xu C, Du Y, et al. Effect of boric acid concentration on the arc stability in underwater wet welding. J Mater Process Technol. 2016;229:244-252. doi:10.1016/j.jmatprotec.2015.09.028
[121] Rowe M, Liu S. Recent developments in underwater wet welding. Sci Technol Weld Join. 2012;6(6):387-396. doi:10.1179/136217101322910560
[122] Xu C, Guo N, Zhang X, Jiang H, Chen H, Feng J. In situ X-ray imaging of melt pool dynamics in underwater arc welding. Mater Des. 2019;179:107899. doi:10.1016/j.matdes.2019.107899
[123] Guo N, Fu Y, Xing X, Liu Y, Zhao S, Feng J. Underwater local dry cavity laser welding of 304 stainless steel. J Mater Process Technol. 2018;260:146-155. doi:10.1016/j.jmatprotec.2018.05.025
[124] Huang ZY, Luo Z, Ao S, Cai YC. Underwater laser weld bowing distortion behavior and mechanism of thin 304 stainless steel plates. Opt Laser Technol. 2018;106:123-135. doi:10.1016/j.optlastec.2018.03.025
[125] Guo N, Xing X, Zhao H, Tan C, Feng J, Deng Z. Effect of water depth on weld quality and welding process in underwater fiber laser welding. Mater Des. 2017;115:112-120. doi:10.1016/j.matdes.2016.11.044
[126] Zhang X, Chen W, Ashida E, Matsuda F. Relationship between weld quality and optical emissions in underwater Nd: YAG laser welding. Opt Lasers Eng. 2004;41(5):717-730. doi:10.1016/S0143-8166(03)00031-9
[127] Wen X, Jin G, Cui X, et al. Underwater wet laser cladding on 316L stainless steel: A protective material assisted method. Opt Laser Technol. 2019;111:814-824. doi:10.1016/j.optlastec.2018.09.022
[128] Zhang X, Ashida E, Shono S, Matsuda F. Effect of shielding conditions of local dry cavity on weld quality in underwater Nd:YAG laser welding. J Mater Process Technol. 2006;174(1- 3):34-41. doi:10.1016/j.jmatprotec.2004.12.009
[129] Antonov AA, Yakovlev YA, Ammosov GG, Kornilova ZG. Investigation of the welded joints of siphon pipes of the underwater crossing of main oil pipeline. Procedia Struct Integr. 2020;30:6-10. doi:10.1016/j.prostr.2020.12.002
[130] Gu C, Lian J, Bao Y, Münstermann S. Microstructure-based fatigue modelling with residual stresses: Prediction of the microcrack initiation around inclusions. Mater Sci Eng A. 2019;751:133-141. doi:10.1016/j.msea.2019.02.058
[131] Dong WC, Wen MY, Pang HY, Lu SP. Effect of Post-weld Tempering on the Microstructure and Mechanical Properties in the Simulated HAZs of a High-Strength–High-Toughness Combination Marine Engineering Steel. Acta Metall Sin (English Lett. 2020;33(3):391-402. doi:10.1007/s40195-019-00954-8
[132] Wang Q, Zhao Z, Zhao Y, Yan K, Zhang H. The adjustment strategy of welding parameters for spray formed 7055 aluminum alloy underwater friction stir welding joint. Mater Des. 2015;88:1366-1376. doi:10.1016/j.matdes.2015.09.038
[133] Wang Q, Zhao Z, Zhao Y, Yan K, Liu C, Zhang H. The strengthening mechanism of spray forming Al-Zn-Mg-Cu alloy by underwater friction stir welding. Mater Des. 2016;102:91-99. doi:10.1016/j.matdes.2016.04.036
[134] Mahto RP, Gupta C, Kinjawadekar M, Meena A, Pal SK. Weldability of AA6061-T6 and AISI 304 by underwater friction stir welding. J Manuf Process. 2019;38:370-386. doi:10.1016/j.jmapro.2019.01.028
[135] Zhao Y, Lu Z, Yan K, Huang L. Microstructural characterizations and mechanical properties in underwater friction stir welding of aluminum and magnesium dissimilar alloys. Mater Des. 2015;65:675-681. doi:10.1016/j.matdes.2014.09.046
[136] Wang ZD, Sun GF, Chen MZ, et al. Investigation of the underwater laser directed energy deposition technique for the on-site repair of HSLA-100 steel with excellent performance. Addit Manuf. 2021;39. doi:10.1016/j.addma.2021.101884
[137] Shin JS, Oh SY, Park SK, Park H, Lee J. Improved underwater laser cutting of thick steel plates through initial oblique cutting. Opt Laser Technol. 2021;141. doi:10.1016/j.optlastec.2021.107120
[138] Fu Y, Guo N, Zhu B, Shi X, Feng J. Microstructure and properties of underwater laser welding of TC4 titanium alloy. J Mater Process Technol. 2020;275:116372. doi:10.1016/j.jmatprotec.2019.116372
[139] Hanliang L, Ning L, Xiaojie L, Xin S, Tao S, Zhanguo M. Joining of Zr60Ti17Cu12Ni11 bulk metallic glass and aluminum 1060 by underwater explosive welding method. J Manuf Process. 2019;45:115-122. doi:10.1016/j.jmapro.2019.06.035
[140] Fu Y, Guo N, Zhou C, Wang G, Feng J. Investigation on in-situ laser cladding coating of the 304 stainless steel in water environment. J Mater Process Technol. 2021;289. doi:10.1016/j.jmatprotec.2020.116949
[141] Krishnan K, Gauni S, Manimegalai CT, Malsawmdawngliana V. Ambient noise analysis in underwater wireless communication using laser diode. Opt Laser Technol. 2019;114:135-139. doi:10.1016/j.optlastec.2018.12.041
[142] Feng X, Cui X, Zheng W, et al. Effect of the protective materials and water on the repairing quality of nickel aluminum bronze during underwater wet laser repairing. Opt Laser Technol. 2019;114:140-145. doi:10.1016/j.optlastec.2019.01.034
[143] Fu Y, Guo N, Zhu B, Shi X, Feng J. Microstructure and properties of underwater laser welding of TC4 titanium alloy. J Mater Process Technol. 2020;275. doi:10.1016/j.jmatprotec.2019.116372
[144] Habib MA, Keno H, Uchida R, Mori A, Hokamoto K. Cladding of titanium and magnesium alloy plates using energy-controlled underwater three layer explosive welding. J Mater Process Technol. 2015;217:310-316. doi:10.1016/j.jmatprotec.2014.11.032
[145] Xiong J, Yang X, Lin W, Liu K. Microstructural characteristics and mechanical heterogeneity of underwater wet friction taper plug welded joints for low-alloy pipeline steel. Mater Sci Eng A. 2017;695:279-290. doi:10.1016/j.msea.2017.04.036
[146] Xiong J, Yang X, Lin W, Liu K. Evaluation of inhomogeneity in tensile strength and fracture toughness of underwater wet friction taper plug welded joints for low-alloy pipeline steels. J Manuf Process. 2018;32:280-287. doi:10.1016/j.jmapro.2018.02.016

[147] Dong S, Han Y, Jia C, et al. Organic adhesive assisted underwater submerged-arc welding. J Mater Process Technol. 2020;284. doi:10.1016/j.jmatprotec.2020.116739
[148] Chen H, Guo N, Zhang Z, Liu C, Zhou L, Wang G. A novel strategy for metal transfer controlling in underwater wet welding using ultrasonic-assisted method. Mater Lett. 2020;270:127692. doi:10.1016/j.matlet.2020.127692
[149] Yang D, Huang Y, Fan J, Jin M, Peng Y, Wang K. Effect of N2 content in shielding gas on formation quality and microstructure of high nitrogen austenitic stainless steel fabricated by wire and arc additive manufacturing. J Manuf Process. 2021;61:261-269. doi:10.1016/j.jmapro.2020.11.020
[150] Ambroziak A, Gul B. Investigations of underwater FHPP for welding steel overlap joints. Arch Civ Mech Eng. 2007;7(2):67-76. doi:10.1016/S1644-9665(12)60212-X

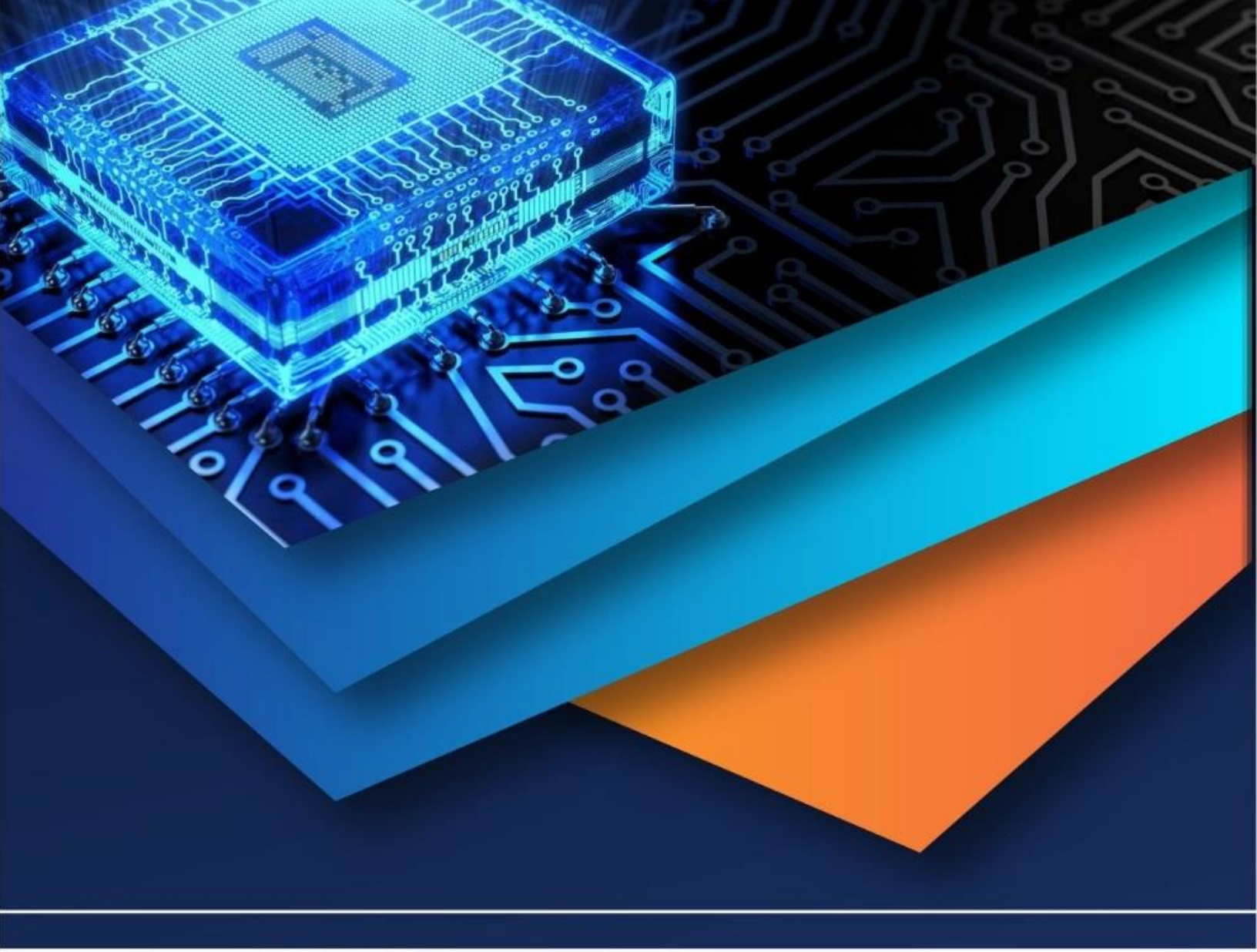

10.22214/IJRASET

45.98

IMPACT FACTOR: 7.129

IMPACT FACTOR: 7.429

INTERNATIONAL JOURNAL FOR RESEARCH

IN APPLIED SCIENCE & ENGINEERING TECHNOLOGY